Research Square

Preprints are preliminary reports that have not undergone peer review.
They should not be considered conclusive, used to inform clinical practice,
or referenced by the media as validated information.

Engineering Mycobacterium neoaurum as a Whole-Cell Platform for Functional Expression of Membrane-Bound 5α-Reductase and Efficient Biosynthesis of 5α-Androstane-3,17-Dione

Shikui Song

sksong@xjnu.edu.cn

Xinjiang Normal University

Lu Zhang

Xinjiang Normal University

Xirenayi Tuergong

Xinjiang Normal University

Zihan Ding

Xinjiang Normal University

Qianqian Ma

Xinjiang University

Xiyao Cheng

Guangxi University

Yajun Duan

University of Science and Technology of China

Zhengding Su

Xinjiang University

Research Article

Keywords: 5α-androstene-3,17-dione, 4-androstene-3,17-dione, 5α-reductase, whole-cell biocatalysis, Mycobacterium neoaurum

Posted Date: November 9th, 2026

DOI: https://doi.org/10.21203/rs.3.rs-10992784/v1

License: This work is licensed under a Creative Commons Attribution 4.0 International License.
Read Full License

Additional Declarations: No competing interests reported.

Engineering *Mycobacterium neoaurum* as a Whole-Cell Platform for Functional Expression of Membrane-Bound 5α-Reductase and Efficient Biosynthesis of 5α-Androstane-3,17-Dione

Shikui Song[1,2*], Lu Zhang[2], Xirenayi·Tuergong[2], Zihan Ding[2], Qianqian Ma[3], Xiyao Cheng[4], Yajun Duan[5] and Zhengding Su[3*]

[1]College of Future Energy and Environmental Engineering, Xinjiang Normal University, Urumqi 830054, China;

[2]Xinjiang Key Laboratory of Special Species Conservation and Regulatory Biology, College of Life Science, Xinjiang Normal University, Urumqi 830054, China;

[3]Institute of Materia Medica, School of Pharmaceutical Sciences, Xinjiang University, Urumqi, Xinjiang, 830017, China;

[4]School of Light Industry and Food Engineering, Guangxi University, Nanning, Guangxi, 530004, China.

[5]Department of Cardiology, The First Affiliated Hospital of USTC, Division of Life Sciences and Medicine, University of Science and Technology of China, Hefei, China.

[*]**To whom correspondence should be addressed:** Zhengding Su, Email: james_su@xju.edu.cn, Tel.: 86-156-23901978, ORCID iD: 0000-0003-3558-001X and Shikui Song, Email: sksong@xjnu.edu.cn, ORCID iD: 0009-0005-9795-4859.

Abstract

5α-Androstane-3,17-dione (5α-AD) is an important steroidal active pharmaceutical intermediate and a precursor for the synthesis of multiple high-value steroid drugs. Conventional 5α-AD production relies largely on chemical synthesis, whereas microbial routes based on sterol side-chain degradation often suffer from low titers, long conversion cycles, and formation of unwanted by-products. NADPH-dependent steroid 5α-reductase (TdSRD5A) from *Treponema denticola* catalyzes the direct reduction of 4-androstene-3,17-dione (4-AD) to 5α-AD. In this work, the TdSRD5A was codon-optimized and functionally expressed in the steroid-transforming chassis *Mycobacterium neoaurum* HGMS6. Recombinant *M. neoaurum*/TdSRD5A cells exhibited high selectivity for converting 4-AD to 5α-AD. Fusion of the LpqH signal peptide to the N terminus of TdSRD5A further improved catalytic activity by approximately 2.4-fold, indicating that membrane-associated localization is beneficial for enzyme function. A whole-cell catalytic system based on *M. neoaurum*/LpqH-TdSRD5A was then developed and optimized. Under optimized conditions, this system produced 19.2 ± 0.4 g/L 5α-AD from 20 g/L 4-AD, representing, to our knowledge, the highest reported 5α-AD titer achieved by bioconversion. Importantly, the process required no exogenous NADPH and generated no detectable by-products. These findings establish recombinant *M. neoaurum* as an effective host for expressing membrane-bound steroid 5α-reductase and provide a promising green biocatalytic platform for industrial 5α-AD production and broader steroid biotransformation applications.

Keywords: 5α-androstene-3,17-dione; 4-androstene-3,17-dione; 5α-reductase; whole-cell biocatalysis; *Mycobacterium neoaurum*.

Introduction

Steroid drugs possess important anti-inflammatory, antiviral, anti-infective, endocrine-regulating and other pharmacological activities, and they remain indispensable in modern medicine [1, 2]. Steroid intermediates are also valuable starting materials for the synthesis of plant hormones and other bioactive compounds [3, 4]. Among these intermediates, steroids containing a 3-oxo-Δ^4 structure can be converted by steroid 5α-reductases into the corresponding 3-oxo-5α-reduced steroids, which participate in key physiological processes associated with benign prostatic hyperplasia, alopecia, prostate cancer, and related androgen-dependent disorders [5-7]. 5α-Androstane-3,17-dione (5α-AD) is a valuable steroidal active pharmaceutical intermediate that can be used to synthesize high-value steroid hormones and derivatives, including dihydrotestosterone, stanozolol, methenolone and androsterone [8, 9]. At present, industrial 5α-AD production is still dominated by chemical synthesis, which often requires multiple steps and may generate environmental burdens [10]. Biological preparation of 5α-AD has attracted increasing interest, but efficient and selective biocatalytic routes remain limited.

Steroid 5α-reductases catalyze the NADPH-dependent reduction of 3-oxo-Δ^4 steroids, including 4-androstene-3,17-dione (4-AD), testosterone and progesterone [11-13]. These enzymes are widespread in mammals and have also been identified in several prokaryotes [14-16]. Structural studies indicate that steroid 5α-reductases are membrane proteins composed of multiple transmembrane segments [16, 17]. Although heterologous expression of 5α-reductase has enabled the biosynthesis of certain reduced steroid products, low enzyme activity and poor membrane-protein expression frequently limit product titers [18, 19]. Recently, Lu et al reported a *Prevotellaceae* 5α-reductase (5αRed-9) that reduces 4-AD with >99% de and a space-time yield of 13.3 g

L^{-1} d^{-1} in *E. coli* [20]. While this work demonstrates that high-activity prokaryotic 5α-reductases can be obtained, the *E. coli* host lacks the native steroid uptake and metabolic machinery characteristic of actinobacteria and may face substrate mass-transfer limitations for hydrophobic steroids in whole-cell biotransformation. By contrast, *M. neoaurum* is a well-established industrial steroid-transforming host with innate capabilities for steroid uptake, intracellular trafficking and tolerance to high substrate loadings [21], whereas *E. coli* lacks the native steroid uptake machinery of actinobacterial hosts, which may limit whole-cell biotransformation of hydrophobic steroids. Despite these advantages, the efficient expression of heterologous 5α-reductases and process development for 4-AD reduction in *M. neoaurum* remain underexplored. Therefore, this study aimed to develop an efficient *M. neoaurum*-based whole-cell platform for the selective conversion of 4-AD to 5α-AD.

M. neoaurum strains are widely used industrial chassis for steroid biotransformation because they efficiently degrade phytosterols and accumulate androstenedione intermediates [22-24]. Their lipid-rich cell envelope facilitates the uptake and export of hydrophobic steroid molecules, making mycobacteria particularly suitable for whole-cell steroid conversion [25]. In addition, resting mycobacterial cells can regenerate reducing cofactors, thereby supporting NADPH-dependent reactions without the need for expensive exogenous cofactors [26, 27].

In this study, we developed a green whole-cell process for 5α-AD production by expressing *Treponema denticola* steroid 5α-reductase (TdSRD5A) in the engineered *M. neoaurum* HGMS6 chassis. HGMS6 contains deletions in genes associated with 3-ketosteroid-$\Delta^{1,2}$-dehydrogenation and 3-ketosteroid-9α-hydroxylation, thereby minimizing further degradation of steroid intermediates. To improve membrane localization and catalytic performance, we fused TdSRD5A to the LpqH signal peptide.

The resulting recombinant strain efficiently catalyzed the one-step conversion of 4-AD to 5α-AD with endogenous cofactor regeneration. This work demonstrates that *M. neoaurum* is an effective host for functional expression of membrane-bound steroid 5α-reductase and provides a scalable whole-cell route for 5α-AD production.

Materials and Methods

Chemicals and Biological Materials

4-Androstene-3,17-dione (4-AD), androsta-1,4-diene-3,17-dione (ADD), testosterone (Ts), methyltestosterone (MTs), progesterone (Pro), 22-hydroxy-23,24-bisnorchol-4-ene-3-one (BA) and 5α-androstane-3,17-dione (5α-AD) were purchased from Sigma-Aldrich (Shanghai, China). Phytosterols were purchased from Yunnan Biological Products Co., Ltd. (Yunnan, China). Industrial-grade 2-hydroxypropyl-β-cyclodextrin (HP-β-CD; >98% purity) was supplied by Zhiyuan Biotechnology Co., Ltd. Restriction enzymes and dNTPs were obtained from TaKaRa Co. (Dalian, China). KOD Plus polymerase was purchased from Toyobo (Shanghai, China). Plasmids were purified using a Plasmid Purification Kit from Tiangen (Beijing, China). PCR products were purified using an agarose gel purification kit (Qiagen, USA). All other molecular biology reagents were of the highest available grade and were obtained from Sigma-Aldrich (Shanghai, China) or Thermo Scientific (Shanghai, China).

Strains and plasmids

Mycobacterium neoaurum HGMS6 (HGMS2$^{\Delta kstd1/\Delta kshA/\Delta kshB}$), which was previously constructed by deleting the *kstd1*, *kshA* and *kshB* genes from the wild-type strain *M. neoaurum* HGMS2, was used as the parental strain for subsequent experiments.

All mutants were generated by introducing pMV261-based overexpression plasmids into HGMS6. The plasmids used in this study are listed in **Supplementary Table S1**, and all plasmid constructs were verified by DNA sequencing. The primers used for plasmid construction are listed in **Supplementary Table S2**. The strains used in this study are provided in **Supplementary Table S3**.

Sequence and structural analysis of TdSRD5A

TdSRD5A was first characterized using sequence-based bioinformatic analyses. Signal peptide probability and potential cleavage sites were predicted using SignalP 5.0 [28]. Transmembrane topology and the number of membrane-spanning helices were inferred using DeepTMHMM [29]. To evaluate sequence conservation, homologous sequences were retrieved by BLAST searches against the UniProt database and multiple sequence alignment was performed with Clustal Omega [30]. The alignment was visualized and annotated using ESPript 3.0 [31], which was used to highlight strictly conserved residues and consensus secondary-structure elements.

For three-dimensional structure prediction, the TdSRD5A amino acid sequence was submitted to AlphaFold2 [32] through the ColabFold platform [33]. Prediction was performed using default settings, with MMseqs2 used to generate the input multiple sequence alignment and the AlphaFold2-ptm model used for structure modeling. Five models were generated and ranked according to predicted local distance difference test (pLDDT) scores. The top-ranked model, which showed the highest overall confidence, was retained as the representative structure. The resulting model was further evaluated by Ramachandran plot analysis and used as the structural template for subsequent computational and mutational analyses.

Transformation of pMV261 plasmids into HGMS6 by electroporation

To achieve gene overexpression in HGMS6, the coding sequences of the target genes were individually cloned into the pMV261 vector under the control of the hsp60 promoter, yielding the recombinant plasmids listed in **Supplementary Table S1**. Each construct was first transformed into *E. coli* DH5α competent cells for propagation, and the resulting plasmids were verified by DNA sequencing before electroporation into HGMS6.

Electrocompetent HGMS6 cells were prepared as described previously [34]. For each transformation, 1 μg of sequence-confirmed plasmid was mixed with 100 μL of competent cells and transferred to a pre-chilled 0.2-cm electroporation cuvette. Electroporation was performed using a Gene Electroporation System (SCIENTZ, Ningbo, China) with a single pulse at 2.2 kV, 20 μF and 1 kΩ, resulting in a time constant of approximately 25 ms. Immediately after pulsing, the cell suspension was diluted with 0.5 mL of LB medium and incubated at 30 °C for 2-3 h with gentle shaking. The entire transformation mixture was then spread onto LB agar plates supplemented with 34 μg/mL kanamycin and incubated at 30 °C for 2-3 days. Kanamycin-resistant colonies were selected and verified by PCR using insert-specific primer pairs (**Table S2**). Positive transformants were stored at -80 °C until further use.

Phytosterols biotransformation assay

Phytosterols biotransformation assays were carried out using growing cells of HGMS6^{pMV261}, HGMS6$^{pMV261\text{-}TdSRD5A}$ and HGMS6$^{pMV261\text{-}LpqH\text{-}TdSRD5A}$. Cultures were grown in 250 mL shake flasks containing 50 mL of biotransformation medium composed of yeast extract (15 g/L), glucose (1 g/L), $NaNO_3$ (5.4 g/L), $(NH_4)_2HPO_4$ (0.6 g/L), Tween-80 (0.05%, v/v) and phytosterols (20 g/L). The flasks were incubated at

30 °C and 200 rpm for 5 days. One milliliter samples of fermentation broth were collected every 24 h for metabolite extraction.

Cell culture, harvesting and resting cell bioconversion

Engineered HGMS6 strains were first activated in 3 mL of seed broth in test tubes for 2 days at 30 °C and 200 rpm. The activated cultures were then inoculated at 10% (v/v) into 50 mL of cell growth medium without phytosterols in 250 mL shake flasks. After cultivation for 3 days at 30 °C and 200 rpm, cells were harvested by centrifugation and weighed as wet cell mass. The supernatant was discarded and the cell pellets were either resuspended in 50 mL of PBS buffer (10 mM, pH 7.4) for immediate use or stored as wet cell paste at -20 °C until biotransformation. Resting cell bioconversion using engineered HGMS6 cells was performed under non-sterile conditions in 250 mL shake flasks containing 50 mL of PBS buffer (10 mM, pH 7.4). Unless otherwise specified, the reaction mixture contained 10 g/L wet cells, 20 g/L 4-AD, HP-β-CD at a 1:1 mass ratio relative to 4-AD and Tween-80 (0.05%, v/v). The flasks were incubated at 30 °C and 200 rpm. Bioconversion reactions were performed in triplicate.

The optimization procedure was performed as follows. Different HP-β-CD/4-AD mass ratios (0:1, 0.5:1, 1:1, 1.5:1, 2:1, 2.5:1 and 3:1) were tested to determine the optimal HP-β-CD concentration. Tween-80 concentrations ranging from 0 to 1.5% (v/v) were evaluated to further improve 4-AD conversion efficiency. Different 4-AD concentrations (20, 40, 60, 80 and 100 g/L) were added during cell cultivation as an inducer to identify the condition that yielded the highest resting-cell activity. Multilevel analyses of resting-cell loading and substrate concentration were then performed to maximize the space-time yield of 5α-AD.

Confocal microscopy

Cells expressing the fluorescent fusion protein were harvested at mid-exponential phase, washed twice with PBS and immobilized on agarose pads (1.5% agarose in PBS). Images were acquired using an Olympus FV3000 confocal laser scanning microscope (Olympus, Japan) equipped with a 100 × oil immersion objective (NA 1.40). Excitation was performed at 488 nm for GFP and emission was collected at 500-550 nm. Images were processed using Olympus FV31S-SW software and ImageJ.

Product isolation and purification

After completion of the biotransformation, the whole-cell culture was extracted three times with an equal volume of ethyl acetate. The combined organic layers were dried over anhydrous Na_2SO_4, filtered and concentrated under reduced pressure to afford the crude product. The crude product was purified by silica gel column chromatography (200-300 mesh silica gel; column: φ2.5 × 30 cm; eluent: petroleum ether/ethyl acetate = 4:1, v/v). Fractions containing the target compound (monitored by TLC) were combined and evaporated to dryness under reduced pressure to afford 5α-AD as a white solid.

TLC analysis

TLC was performed on 0.25-mm fluorescent silica gel G plates (Silica gel 254; Qingdao Haiyang Chemical Co., China) using petroleum ether/ethyl acetate (1:1, v/v) as the mobile phase. Sample extracts were spotted onto the plates in 5-μL aliquots. Reaction products were visualized under ultraviolet (UV) light. When necessary, TLC plates were stained with 20% sulfuric acid and heated at 100 °C for 10 min to detect compounds that were not visible under UV light.

HPLC analysis

HPLC analysis was performed on a C18 reverse-phase SunFire column (5 μm, 4.6 × 150 mm; Waters, USA) maintained at 30 °C using a Waters HPLC system equipped with a UV detector. Samples were diluted to an appropriate concentration (approximately 1 mg/mL) with methanol and filtered through 0.22 μm pore-size membranes. HPLC separation was performed using acetonitrile/water (60:40, v/v) as the mobile phase at a flow rate of 1 mL/min. Analytes were detected by UV absorbance at 254 nm or 200 nm.

Results and discussion

5α-reductase is predicted to be a seven-transmembrane protein

Sequence alignment showed that TdSRD5A from *T. denticola* shares relatively low overall amino acid identity (approximately 37%) with the steroid 5α-reductase from *Proteobacteria bacterium*, whereas the predicted catalytic region is more conserved, with approximately 55% identity (**Fig. 1a**). The TdSRD5A structural model generated by AlphaFold2 showed high similarity to the reported crystal structure of PbSRD5A (PDB: 7C83) (**Fig. 1b, c**). Topology analysis predicted that TdSRD5A contains seven transmembrane segments, with the N terminus located on the periplasmic side and the C terminus exposed to the cytosolic side, consistent with DeepTMHMM prediction (**Fig. S1a**). SignalP-5.0 analysis suggested that native TdSRD5A lacks a clear signal peptide (**Fig. S1b**). Conserved residues implicated in NADPH binding and steroid reduction were also identified, including the key tyrosine and glutamate residues within the hydrophobic substrate-binding pocket (**Fig. 1a**). These features support the classification of TdSRD5A as a membrane-bound NADPH-dependent steroid 5α-reductase capable of reducing the 3-oxo-Δ^4 steroid substrate testosterone (**Fig. 1d**).

Expression and activity analysis of TdSRD5A

Because TdSRD5A is predicted to be a multi-pass membrane protein, we first evaluated its heterologous expression in two hosts, *Escherichia coli* and *Mycobacterium*. The TdSRD5A gene was codon-optimized for *E. coli* and cloned into pET20b and pRSV-MBP vectors, generating pET20b-TdSRD5A and pRSV-MBP-TdSRD5A, respectively (**Fig. S2a-b**). However, transformation of pET20b-TdSRD5A into *E. coli* yielded only a small number of slow-growing colonies, whereas the empty pET20b control produced normal growth (**Fig. S2c**). Furthermore, we sequenced single colonies to verify TdSRD5A and induced protein expression under optimal expression conditions. However, no bands of TdSRD5A 45% on SDS-PAGE (**Fig. S2d, Lanes 1-2**). To boost protein expression, the MBP tag was added to the N-terminus of the TdSRD5A gene (**Fig. S2b**). It was discovered that with 0.3 mM IPTG induction for 6 hours at 37°C, the protein expression conditions could be improved to provide greater protein expression levels (**Fig. S2d, Lanes 3-4**). Although the MBP fusion improved detectable expression after induction with 0.3 mM IPTG for 6 h at 37 °C, no 5α-AD was detected when 4-AD was incubated with either the soluble or precipitated fraction of disrupted *E. coli* cells. Instead, only trace amounts of ADD were observed (**Fig. 2a, lanes 1-3**). In the present study, functional expression of TdSRD5A was not achieved in *E. coli* under the conditions tested; the MBP-TdSRD5A fusion protein was detected in the soluble fraction but showed no detectable activity toward 3-oxo-Δ^4 substrates. Notably, Lu et al recently achieved functional expression of a bacterial 5α-reductase (5αRed-9) in *E. coli* [20], indicating that *E. coli* can support at least some prokaryotic 5α-reductases. The discrepancy may reflect enzyme-specific folding requirements, vector design or strain background rather than a general host limitation. Nevertheless, expression of TdSRD5A in *M. neoaurum* enabled efficient whole-cell conversion of 4-

AD to 5α-AD, benefiting from the host's native steroid uptake and metabolic capabilities.

We next optimized TdSRD5A codons for mycobacterial expression and introduced the construct into *M. neoaurum* HGMS6. Activity assays using different cellular fractions revealed that 5α-AD was clearly detected in the whole-cell lysate. After removal of cell debris and other precipitates from the lysate, no 5α-AD was observed in the supernatant fraction, while a trace amount of ADD was detected in the reaction product of the supernatant (**Fig. 2a, lane 7**). In contrast, the precipitated debris suspension fraction exhibited substantial 5α-AD accumulation, with nearly complete conversion of 4-AD within 12 h (**Fig. 2a, Lanes 6 and 8**). These findings indicate that mycobacteria can functionally express TdSRD5A and that the active enzyme is mainly associated with the membrane-containing cell-debris fraction. To further improve expression and membrane localization, the signal peptide and linker region of the mycobacterial lipoprotein LpqH were fused to the N terminus of TdSRD5A (**Fig. S3b-3c**). Recombinant plasmids pMV261-TdSRD5A and pMV261-LpqH-TdSRD5A were introduced into HGMS6 to generate HGMS6$^{p261\text{-}TdSRD5A}$ and HGMS6$^{p261\text{-}LpqH\text{-}TdSRD5A}$ (**Fig. S3a**). Using 4-AD as substrate, HGMS6$^{p261\text{-}LpqH\text{-}TdSRD5A}$ showed approximately 2.4-fold higher activity than HGMS6$^{p261\text{-}TdSRD5A}$, whereas the vector-control strain HGMS6^{p261} showed no detectable 5α-reductase activity (**Fig. 2b**). The molecular mechanism underlying this enhancement remains unclear. Although SDS-PAGE analysis suggested that the LpqH fusion may enhance TdSRD5A expression and/or membrane association **(Fig. S3d)**, the relative contributions of these two factors could not be distinguished from the present data and warrant further quantitative analysis.

To determine the intracellular localization of TdSRD5A, three GFP-based strains were constructed: HGMS6$^{p261\text{-}gfp}$, HGMS6$^{p261\text{-}TdSRD5A\text{-}gfp}$ and HGMS6$^{p261\text{-}LpqH\text{-}TdSRD5A\text{-}gfp}$.

The non-fluorescent strain HGMS6$^{p261\text{-}LpqH\text{-}TdSRD5A}$ was used as a background control for confocal imaging. Confocal microscopy showed strong fluorescence in GFP-expressing cells and enabled visualization of TdSRD5A and LpqH-TdSRD5A fusion proteins **(Fig. 2c-f)**. The images shown are representative of multiple independent observations; quantitative analysis was not performed. It should be noted that the enzymatic activity of the GFP-fused proteins was not directly verified in this study. Although the GFP-tag did not prevent membrane localization, the possibility that the fusion proteins are catalytically inactive cannot be excluded. Therefore, the localization data alone do not establish a direct link between membrane association and catalytic function and should be interpreted with caution. Nevertheless, these results are consistent with the notion that membrane association is important for TdSRD5A function, although further validation would be required to strengthen this conclusion.

Phytosterol fermentation using the HGMS6$^{p261\text{-}LpqH\text{-}TdSRD5A}$ mutant

Because mycobacterial expressed TdSRD5A exhibited high activity toward 4-AD, we next examined whether the recombinant strain could directly convert phytosterols to 5α-AD in a one-pot fermentation process. HGMS6 was used as the control strain, and phytosterol fermentation was performed in 250 mL flasks containing 50 mL fermentation medium (see "**Materials and methods**"). In the control HGMS6 strain, phytosterols were efficiently converted to 4-AD, reaching a conversion rate of 52.3% after 7 days with 5 g/L phytosterol, but no 5α-AD was detected **(Fig. 3a)**. In contrast, the HGMS6$^{p261\text{-}LpqH\text{-}TdSRD5A}$ mutant produced only a small amount of 5α-AD (<1%) and the overall phytosterols conversion efficiency decreased markedly, with less than 20% 4-AD accumulation in the fermentation broth (**Fig. 3b**). Given that 5α-AD and 4-AD together accounted for less than 21% of the initial substrate, the majority of phytosterols

was presumably not consumed, although residual substrate was not directly quantified. This suggests that the reduced product formation primarily resulted from impaired substrate uptake or metabolism.

This result is lower than the 86.4% conversion reported by Zhao et al using the same enzyme in the same host [22]. The discrepancy may be attributed to differences in experimental parameters, including substrate loading, phytosterol solubilization strategy, culture conditions or the relative expression levels of TdSRD5A and the NADPH-regenerating enzymes. When 4-AD was supplied directly as the substrate in the whole-cell transformation system, 5α-AD production increased dramatically with no detectable by-products. This result demonstrates that the engineered strain possesses high TdSRD5A activity and sufficient endogenous NADPH regeneration capacity and that the bottleneck in the direct phytosterol-to-5α-AD route likely resides in the coupling efficiency between the endogenous sterol degradation pathway and the heterologous reductase under the specific conditions employed.

Application of TdSRD5A in whole-cell transformation and product identification

The poor aqueous solubility of steroids limits substrate availability during biotransformation, whereas high concentrations of organic solvents can damage whole-cell biocatalysts. Hydroxypropyl-β-cyclodextrin (HP-β-CD) is widely used to improve steroid solubility because of its hydrophilic exterior and hydrophobic inner cavity. Tween-80 can also disperse hydrophobic steroid substrates and improve mass transfer. Therefore, HP-β-CD and Tween-80 were added to the resting-cell transformation system to enhance the contact between 4-AD and recombinant mycobacterial cells. Both HGMS6$^{p261\text{-}TdSRD5A}$ and HGMS6$^{p261\text{-}LpqH\text{-}TdSRD5A}$ showed clear 4-AD reduction activity compared with the negative control **(Fig. 4a)**. With an initial 4-AD

concentration of 20 g/L, HGMS6$^{p261\text{-}TdSRD5A}$ converted approximately 45% of 4-AD to 5α-AD within 4 days, whereas HGMS6$^{p261\text{-}LpqH\text{-}TdSRD5A}$ was more than twice as efficient. HPLC and TLC analyses confirmed that 5α-AD was the major product, as demonstrated by comparison with authentic 4-AD and 5α-AD standards **(Fig. 4b)**.

For product isolation, the whole-cell culture of HGMS6$^{p261\text{-}LpqH\text{-}TdSRD5A}$ was extracted with ethyl acetate and the crude product was purified by silica gel column chromatography. The isolated product was confirmed as 5α-AD by LC/MS and NMR analysis. LC/MS gave a protonated molecular ion $[M+H]^+$ at m/z 289.2, which is consistent with the calculated molecular weight of 5α-AD **(Fig. 4c)**. In the ^{1}H NMR spectrum, the C4 proton signal changed from δ 5.85 in 4-AD to new signals at δ 2.31 and δ 2.06 in 5α-AD and an additional singlet appeared at δ 1.46 **(Fig. S4)**. ^{13}C NMR confirmed that the steroid carbon skeleton was retained **(Fig. S5)**, whereas HSQC and NOESY analyses verified the presence and α-orientation of the C5 hydrogen **(Fig. 4d; Fig. S6)**.

A lag period was observed before the onset of rapid 5α-AD formation **(Fig. 4a)**. Although the underlying cause of this lag was not directly investigated, it may reflect the time required for substrate uptake or cellular adaptation to the reaction conditions, followed by accelerated conversion until substrate depletion. To maintain cell activity during transformation, small amounts of glycerol were added periodically as a carbon source [35, 36]. Glycerol catabolism likely contributed to NADPH regeneration via the pentose phosphate pathway, thereby supporting the sustained activity of TdSRD5A [37]. Therefore, periodic glycerol supplementation may have helped maintain NADPH availability, although intracellular NADPH/$NADP^+$ ratios were not directly measured. In addition, deletion of *the kstd* and *ksh* genes in the HGMS6 chassis blocks the further degradation of phytosterols, thereby reducing NADPH consumption and preserving

intracellular NADPH for the TdSRD5A-catalyzed reduction [38]. Furthermore, the inclusion of HP-β-CD and Tween-80 enhanced the solubilization and dispersion of 4-AD, likely contributing to the improved conversion efficiency by increasing substrate availability.

Optimization of whole-cell transformation conditions

Effects of HP-β-CD and Tween-80

Steroid substrates generally display low water solubility, which restricts their accessibility to whole-cell biocatalysts. We therefore evaluated the effect of different HP-β-CD/4-AD mass ratios on 5α-AD production (**Fig. 5a**). Relative conversion (%) in **Fig. 5a** was calculated by normalizing the 5α-AD titer obtained under each condition to that obtained at an HP-β-CD/4-AD mass ratio of 1:1, which was defined as 100%. 5α-AD production increased with increasing HP-β-CD concentration up to an optimal ratio, but decreased when the HP-β-CD/4-AD mass ratio exceeded 2:1. Excess HP-β-CD may reduce biotransformation efficiency by sequestering 4-AD and limiting access to the enzyme. The optimal HP-β-CD/4-AD mass ratio was 0.5:1, at which 5α-AD production reached 2.76 g/L. This ratio was used in subsequent experiments.

Tween-80 was also evaluated as a dispersing agent. As shown in **Fig. 5b**, relative conversion (%) was calculated by normalizing the 5α-AD titer obtained under each condition to that obtained at a Tween-80 concentration of 0.5% (v/v), which was defined as 100%. 4-AD conversion increased with Tween-80 concentration and reached a maximum at 0.1%. Above this concentration, conversion gradually decreased, probably because excessive Tween-80 disrupts the cell envelope or destabilizes membrane-associated proteins, thereby impairing TdSRD5A activity.

Effect of substrate concentration

To further increase 5α-AD production, we tested different initial 4-AD concentrations in the resting-cell biotransformation system **(Fig. 5c)**. During the 6-day conversion period, 20 g/L 4-AD was almost completely converted by the 3rd day, producing 18.3 g/L 5α-AD. At 40 g/L 4-AD, approximately 38.1 g/L 5α-AD was obtained by the 4th day. Increasing the substrate concentration to 60 g/L yielded 56.8 g/L 5α-AD, indicating that high substrate loading is feasible in this system. However, further increases in 4-AD concentration did not improve conversion efficiency, likely because the reaction mixture approached the solubility limit and high substrate concentrations partially inhibited TdSRD5A activity. Therefore, 60 g/L 4-AD was selected for subsequent optimization.

Effect of biomass

The effect of recombinant HGMS6$^{p261\text{-}LpqH\text{-}TdSRD5A}$ biomass on the conversion of 4-AD to 5α-AD was then examined (**Fig. 5d**). The conversion efficiency improved with increasing biomass loading. At a wet cell concentration of 10 g/L, the conversion rate remained below 50% after 30 h of reaction, which was the lowest among all tested groups. In contrast, the highest conversion efficiency was achieved with 110 g/L wet cells, reaching over 40% at 10 h and exceeding 90% at 30 h. The enhanced conversion at higher cell densities is attributed to more frequent effective collisions between steroid molecules and cells, thereby accelerating substrate turnover. Notably, no inhibitory effect on substrate conversion was observed at the highest tested cell density, suggesting that this concentration may not yet reach the upper limit of cell tolerance in the transformation system and thus did not significantly affect mass transfer.

Under a substrate concentration of 20 g/L, the conversion of other steroid

substrates was examined at a wet-cell/substrate mass ratio of 1:2. The 5α-AD titer increased with reaction time and reached 19.2 ± 0.4 g/L within 50 h, with nearly complete conversion of 4-AD and no detectable by-products (**Fig. S7a**). Substrate-scope analysis showed that TdSRD5A also reduced other steroid substrates. Progesterone displayed approximately 20% higher catalytic activity than 4-AD, whereas the activities toward BA and 4-AD were similar. Catalytic activity toward testosterone and methyltestosterone was approximately 5-fold and 2.5-fold lower, respectively, than that toward 4-AD (**Fig. S7b**).

Conclusions

In this study, we established a mycobacterium-based whole-cell biocatalytic platform for the efficient production of 5α-AD by expressing *T. denticola* steroid 5α-reductase in *M. neoaurum* HGMS6. While functional expression of TdSRD5A was not achieved in *E. coli* under the conditions tested, it was successfully expressed in mycobacterial cells. Fusion of the LpqH signal peptide further enhanced TdSRD5A activity, likely by improving membrane localization and orientation. Optimization of co-solvent composition, substrate concentration and biomass enabled efficient conversion of 4-AD to 5α-AD. Under optimized conditions, 20 g/L 4-AD was converted to 19.2 ± 0.4 g/L 5α-AD within 50 h, with no detectable by-products and without addition of exogenous NADPH. To our knowledge, this represents the highest reported 5α-AD production titer by biotransformation **(Table S4)**. These findings provide an efficient and environmentally friendly route for 5α-AD production and demonstrate the potential of engineered *M. neoaurum* as a chassis for membrane-enzyme-driven steroid biocatalysis.

Supplementary information: E-supplementary data of this word can be found in online version of the paper.

Ethics Declarations

Not applicable.

Consent for publication

Not applicable.

Availability of data and material

All data generated and analyzed during this study are included in this published article.

Competing interests

The authors declare that they have no conflicts of interest.

Funding

This work was partially supported by the “Tianchi Talents” introduction plan of Xinjiang Uygur Autonomous Region, the Natural Science Foundation of Xinjiang Uygur Autonomous Region (2024D01B63), the Doctoral Research Foundation of Xinjiang Normal University (No. XJNUZBS2421), the National Natural Science Foundation of China to ZDS (22468047) and the Xinjiang University Double-first Rate Initiative Program to ZDS.

Authors' contributions

ZDS, SKS, YJD and XYC designed the research. LZ, XRAY, ZHD, QQM and SKS conducted the experiments. SSK analyzed the data. ZDS and SKS wrote the manuscript. All authors read and approved the manuscript.

Acknowledgements

We thank Jianxin He, Deqiang Lv and Xinlin Dong for their technical assistance.

Author information and affiliations

References

1. Donova MV, Egorova OV: Microbial steroid transformations: current state and prospects. Appl Microbiol Biotechnol 2012, 94**:**1423-1447.
2. Wang XX, Ke X, Liu ZQ, Zheng YG: Rational development of mycobacteria cell factory for advancing the steroid biomanufacturing. World J Microbiol Biotechnol 2022, 38**:**191.
3. Li X, Zhang R, Li J, Liu N, Chen X, Liu Y, et al: Chemo-Enzymatic Strategy for the Efficient Synthesis of Steroidal Drugs with 10alpha-Methyl Group and a Side Chain at C17-Position from Biorenewable Phytosterols. JACS Au 2024, 4**:**1356-1364.
4. Li T, Li C: Quantitative and stereospecific dihydroxylations of δ(5)-steroids: a green synthesis of plant growth hormone intermediates. J Agric Food Chem 2013, 61**:**12522-12530.
5. Azzouni F, Godoy A, Li Y, Mohler J: The 5 alpha-reductase isozyme family: a review of basic biology and their role in human diseases. Adv Urol 2012, 2012**:**530121.
6. Wang Z, Gu B, Sharkey C, Ge R, Olumi AF: SRD5A2 and emerging therapies in androgen-driven disorders. Nature Reviews Urology 2026, 23**:**319-332.
7. Sharifi N: The 5α-androstanedione pathway to dihydrotestosterone in castration-resistant prostate cancer. J Investig Med 2012, 60**:**504-507.
8. Pettit GR, Moser BR, Mendonca RF, Knight JC, Hogan F: The cephalostatins. 22. synthesis of bis-steroidal pyrazine pyrones (1). J Nat Prod 2012, 75**:**1063-1069.
9. Ayan D, Maltais R, Hospital A, Poirier D: Chemical synthesis, cytotoxicity, selectivity and bioavailability of 5alpha-androstane-3alpha,17beta-diol derivatives. Bioorg Med Chem 2014, 22**:**5847-5859.
10. Zhang H, Qiu Z: An efficient synthesis of 5alpha-androst-1-ene-3,17-dione. Steroids 2006, 71**:**1088-1090.
11. Schiffer L, Arlt W, Storbeck KH: 5α-reduction of epitestosterone is catalysed by human SRD5A1 and SRD5A2 and increases androgen receptor transactivation. J

Steroid Biochem Mol Biol 2024, 241:106516.
12. Corbin CJ, Legacki EL, Ball BA, Scoggin KE, Stanley SD, Conley AJ: Equine 5α-reductase activity and expression in epididymis. J Endocrinol 2016, 231:23-33.
13. Samson M, Labrie F, Luu-The V: Sequential transformation of 4-androstenedione into dihydrotestosterone in prostate carcinoma (DU-145) cells indicates that 4-androstenedione and not testosterone is the substrate of 5α-reductase. Horm Mol Biol Clin Investig 2010, 1:67-72.
14. Han Y, Zhuang Q, Ren R: Approach1es for evolutionary, biochemical, and structural analysis of bacterial steroid 5α-reductases. Methods Enzymol 2023, 689:237-261.
15. Glass TL, Saxerud MH, Casper HH: Properties of a 4-ene-3-ketosteroid-5 alpha-reductase in cell extracts of the intestinal anaerobe, Eubacterium sp. strain 144. J Steroid Biochem Mol Biol 1991, 39:367-374.
16. Russell DW, Wilson JD: Steroid 5 alpha-reductase: two genes/two enzymes. Annu Rev Biochem 1994, 63:25-61.
17. Han Y, Zhuang Q, Sun B, Lv W, Wang S, Xiao Q, et al: Crystal structure of steroid reductase SRD5A reveals conserved steroid reduction mechanism. Nat Commun 2021, 12:449.
18. Im SC, Valentín-Goyco J, Peng HM, Auchus RJ: Bacterial expression, purification, and reconstitution of human steroid 5α-reductases in phospholipid liposomes and nanodiscs. Methods Enzymol 2023, 689:263-276.
19. Peng HM, Valentín-Goyco J, Im SC, Han B, Liu J, Qiao J, Auchus RJ: Expression in Escherichia Coli, Purification, and Functional Reconstitution of Human Steroid 5α-Reductases. Endocrinology 2020, 161.
20. Lu C, Wang Y, Zhang R, Chen X, Zhang Z, Qi X, Feng J, Wu Q, Zhu D: A Highly Efficient Enzymatic Method for the Sustainable and Stereoselective Production of 5α-H Key Intermediates for Steroidal Pharmaceuticals. Advanced Synthesis and Catalysis 2026, 368:e70572.
21. Zhao A, Zhang X, Li Y, Wang Z, Lv Y, Liu J, Alam MA, Xiong W, Xu J:

Mycolicibacterium cell factory for the production of steroid-based drug intermediates. Biotechnology Advances 2021, 53:107860.

22. Zhao Y, Shen Y, Ma S, Luo J, Ouyang W, Zhou H, Tang R, Wang M: Production of 5α-androstene-3,17-dione from phytosterols by co-expression of 5α-reductase and glucose-6-phosphate dehydrogenase in engineered Mycobacterium neoaurum. Green Chemistry 2019, 21:1809-1815.

23. Galán B, Uhía I, García-Fernández E, Martínez I, Bahíllo E, de la Fuente JL, Barredo JL, Fernández-Cabezón L, García JL: Mycobacterium smegmatis is a suitable cell factory for the production of steroidic synthons. Microb Biotechnol 2017, 10:138-150.

24. Fernandez-Cabezon L, Galan B, Garcia JL: New Insights on Steroid Biotechnology. Front Microbiol 2018, 9:958.

25. Zhou Y, Wang X, Jia W, Su Z, Cheng X: The Biosynthetic Pathway of Mycolic Acids: Dual-Function Targets for Tuberculosis Therapeutics and Green Steroid Drugs Biomanufacturing. Pharmaceutics 2025, 18.

26. Gao XQ: Enhanced Steroid Metabolites Production by Resting Cell Phytosterol Bioconversion. Chemical and Biochemical Engineering Quarterly 2016, 29:567-573.

27. Ke X, Cui JH, Ren QJ, Zheng T, Wang XX, Liu ZQ, Zheng YG: Rerouting phytosterol degradation pathway for directed androst-1,4-diene-3,17-dione microbial bioconversion. Appl Microbiol Biotechnol 2024, 108:186.

28. Almagro Armenteros JJ, Tsirigos KD, Sønderby CK, Petersen TN, Winther O, Brunak S, von Heijne G, Nielsen H: SignalP 5.0 improves signal peptide predictions using deep neural networks. Nat Biotechnol 2019, 37:420-423.

29. Chen Y, Chen L, Huang S, Yang L, Wang L, Yang F, Huang J, Ding X: Predicting novel biomarkers for early diagnosis and dynamic severity monitoring of human ulcerative colitis. Front Genet 2024, 15:1429482.

30. Sievers F, Wilm A, Dineen D, Gibson TJ, Karplus K, Li W, et al: Fast, scalable generation of high-quality protein multiple sequence alignments using Clustal Omega. Mol Syst Biol 2011, 7:539.

31. Robert X, Gouet P: Deciphering key features in protein structures with the new ENDscript server. Nucleic Acids Res 2014, 42**:**W320-324.
32. Jumper J, Evans R, Pritzel A, Green T, Figurnov M, Ronneberger O, et al: Highly accurate protein structure prediction with AlphaFold. Nature 2021, 596**:**583-589.
33. Mirdita M, Schütze K, Moriwaki Y, Heo L, Ovchinnikov S, Steinegger M: ColabFold: making protein folding accessible to all. Nat Methods 2022, 19**:**679-682.
34. Li X, Chen T, Peng F, Song S, Yu J, Sidoine DN, Cheng X, Huang Y, He Y, Su Z: Efficient conversion of phytosterols into 4-androstene-3,17-dione and its C1,2-dehydrogenized and 9alpha-hydroxylated derivatives by engineered Mycobacteria. Microb Cell Fact 2021, 20**:**158.
35. Lee W-H, Kim M-D, Jin Y-S, Seo J-H: Engineering of NADPH regenerators in Escherichia coli for enhanced biotransformation. Applied Microbiology and Biotechnology 2013, 97**:**2761-2772.
36. Song S, Wang Y, Yu J, Ma Q, Cheng X, Zhang B, Su Z: Knockout of glycerol metabolic pathways enables efficient mycolicibacterial phytosterol conversion using glycerol as cosovlent. Appl Microbiol Biotechnol 2025, 109**:**169.
37. Beste DJ, Bonde B, Hawkins N, Ward JL, Beale MH, Noack S, Nöh K, Kruger NJ, Ratcliffe RG, McFadden J: ^{13}C metabolic flux analysis identifies an unusual route for pyruvate dissimilation in mycobacteria which requires isocitrate lyase and carbon dioxide fixation. PLoS Pathog 2011, 7**:**e1002091.
38. Sun WJ, Wang L, Liu HH, Liu YJ, Ren YH, Wang FQ, Wei DZ: Characterization and engineering control of the effects of reactive oxygen species on the conversion of sterols to steroid synthons in Mycobacterium neoaurum. Metab Eng 2019, 56**:**97-110.

Figure legends

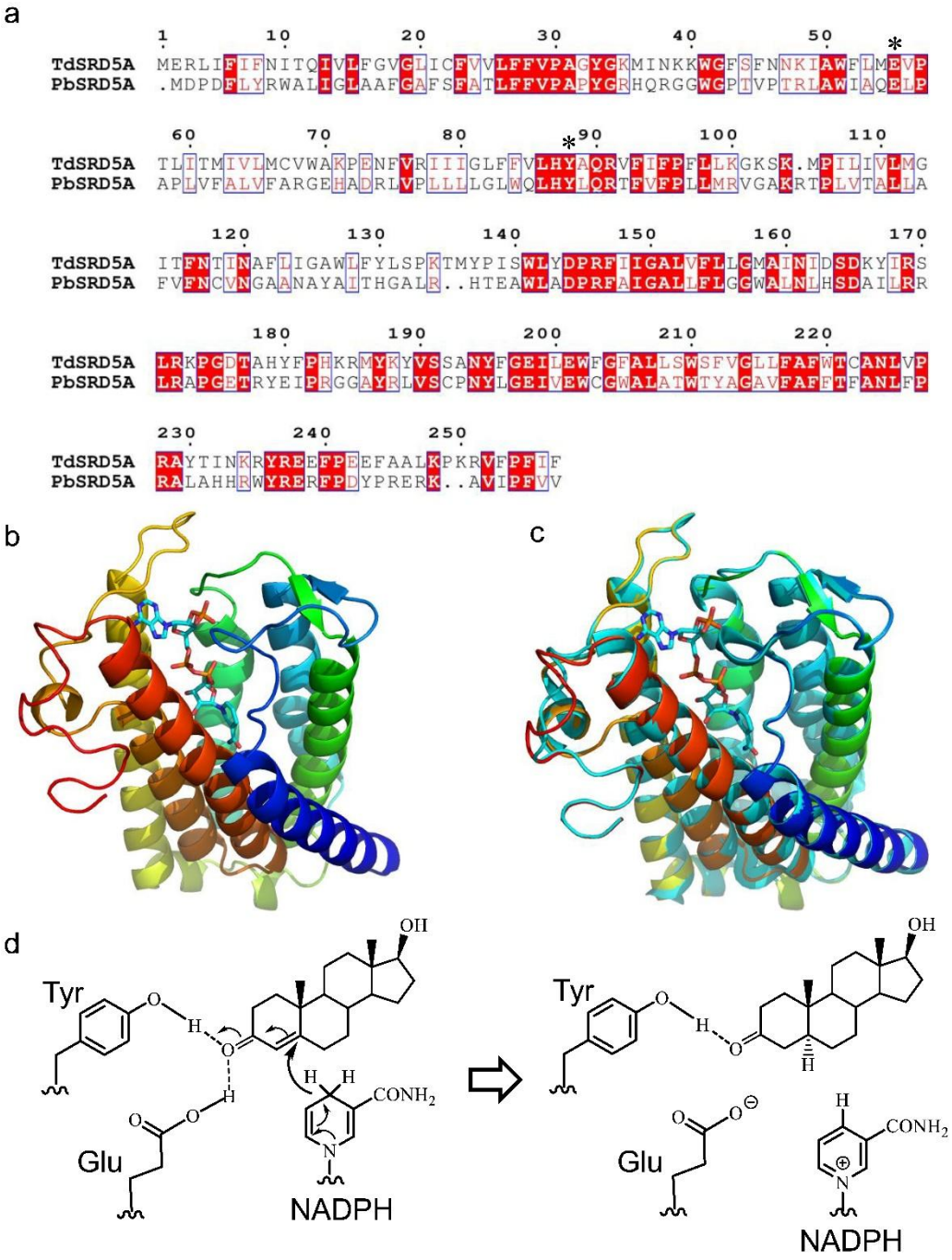


Fig. 1. Amino acid sequence and three-dimensional structure of 5α-reductase. a. Amino acid sequence of TdSRD5A aligned with that of a *Proteobacteria bacterium* strain. **b.** Three-dimensional structure of TdSRD5A predicted using the AlphaFold2 program. **c.** Structure of TdSRD5A (rainbow) superimposed on that from *Proteobacteria bacterium* (PDB: 7C83, cyan). **d.** Schematic diagram of the proposed catalytic mechanism of 5α-reductase.

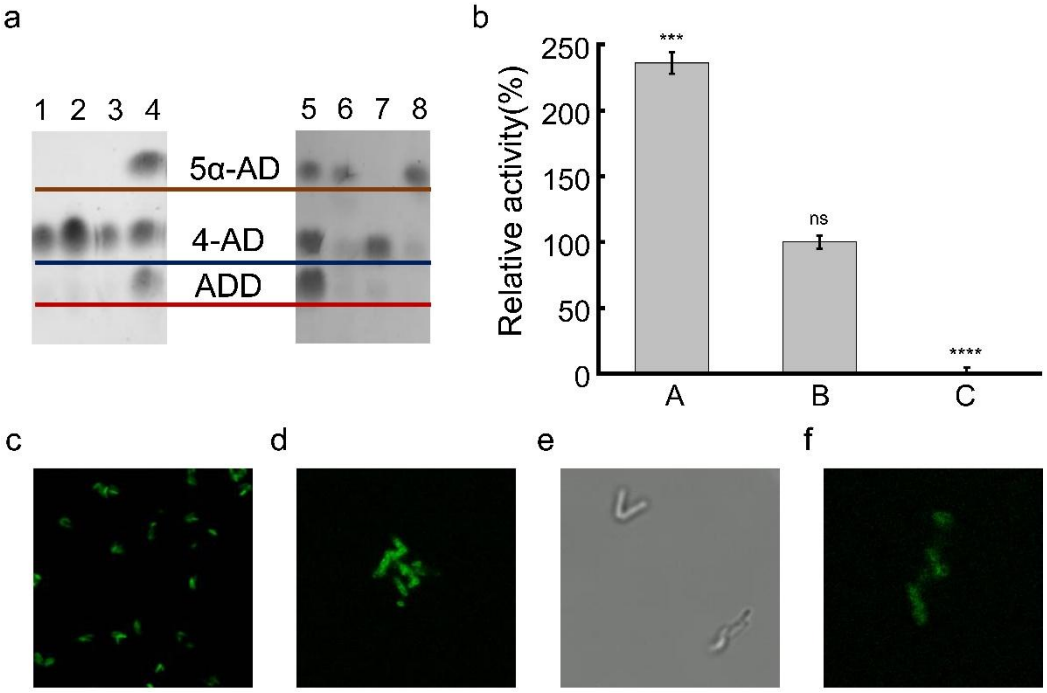


Fig. 2. Functional expression, activity comparison and subcellular localization of TdSRD5A in *M. neoaurum* HGMS6. **a**. TLC analysis of the catalytic activity of TdSRD5A in different cellular fractions of recombinant *E. coli* (left panel) and *M. neoaurum* (right panel). Lanes 4 and 5: standards; Lanes 1 and 8: precipitate suspension; Lanes 2 and 7: supernatant after centrifugation; Lanes 3 and 6: whole-cell lysate. **b.** Comparison of TdSRD5A activities of the recombinant strains. A: HGMS6$^{p261\text{-}LpqH\text{-}TdSRD5A}$; B: HGMS6$^{p261\text{-}TdSRD5A}$; C: HGMS6^{p261} (empty vector control). Data are mean ± SD (n=3). Statistical significance was analyzed by one-way ANOVA followed by Dunnett's test. ***, P<0.001 and ****, P<0.0001 indicate significant differences compared with strain B; ns, not significant. **c–f.** Confocal fluorescence images of strains HGMS6$^{p261\text{-}gfp}$ (**c**), HGMS6$^{p261\text{-}TdSRD5A\text{-}gfp}$ (**d**), and HGMS6$^{p261\text{-}LpqH\text{-}TdSRD5A\text{-}gfp}$ (**f**), and a bright-field image of strain HGMS6$^{p261\text{-}LpqH\text{-}TdSRD5A}$ (**e**).

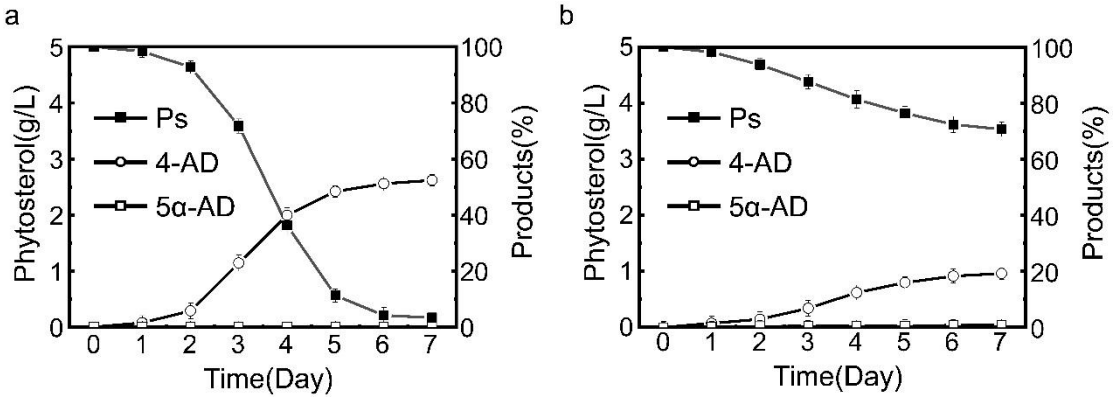


Fig. 3. Phytosterol fermentation by recombinant strains and proposed catalytic mechanism of TdSRD5A. a-b. Phytosterol fermentation time courses of HGMS6 (**a**) and HGMS6$^{p261\text{-}LpqH\text{-}TdSRD5A}$ (**b**). **c.** Proposed catalytic route of TdSRD5A in *M. neoaurum*.

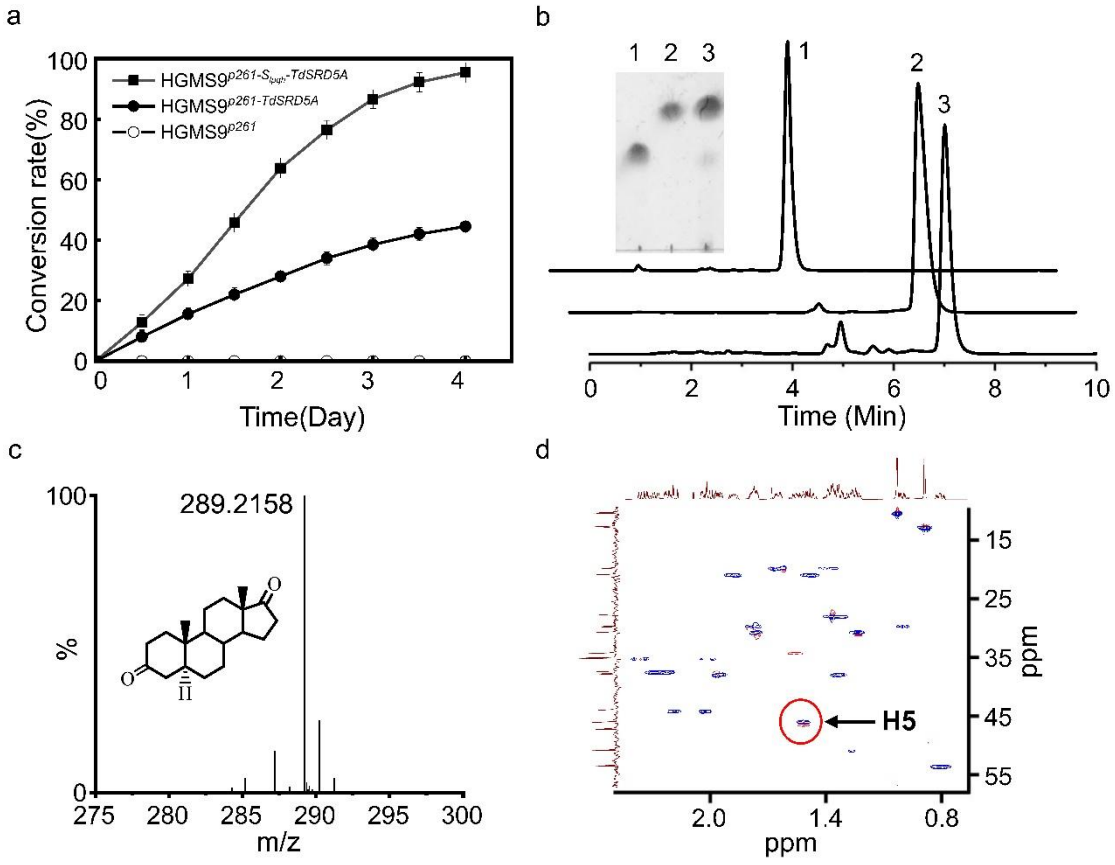


Fig. 4. Whole-cell transformation of 4-AD to 5α-AD and product identification. a. Time course of whole-cell transformation of 4-AD to 5α-AD by recombinant strains. **b–d.** HPLC and TLC analysis (**b**), LC/MS spectrum (**c**), and HSQC spectrum (**d**) of 5α-

AD.

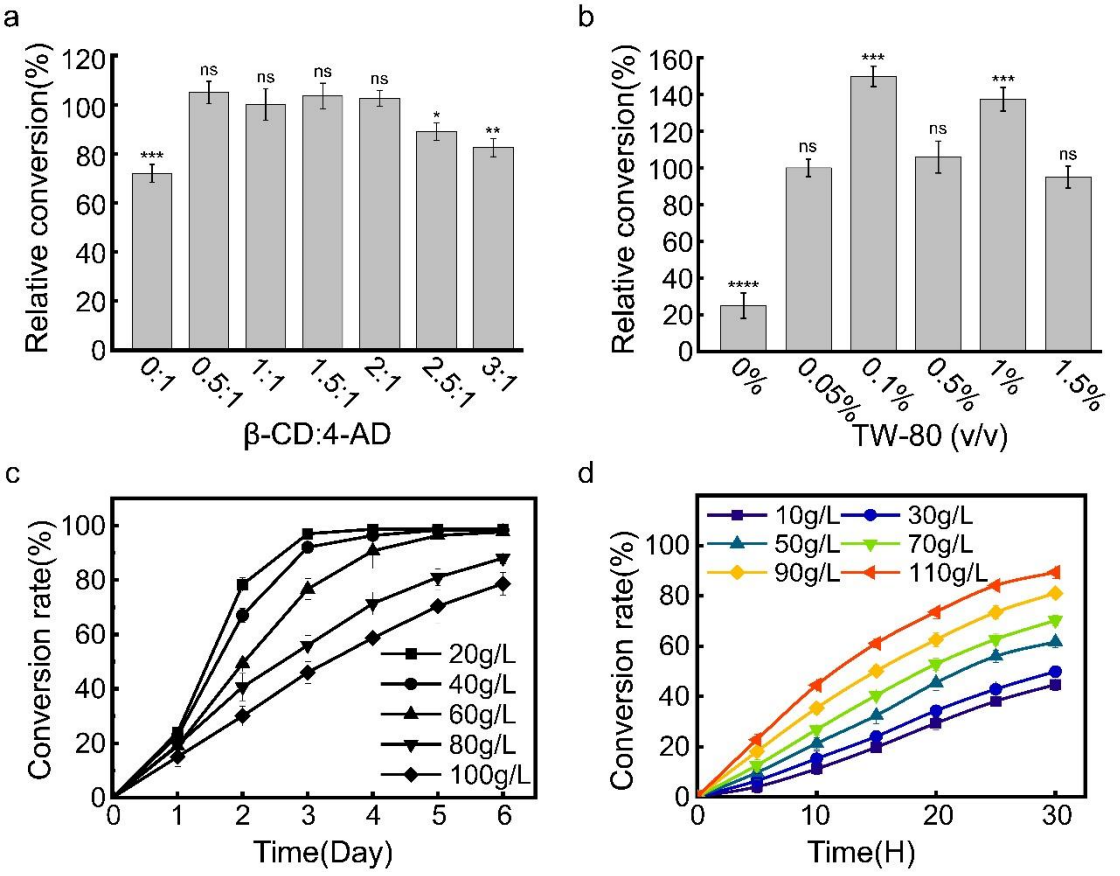


Fig. 5. Optimization of whole-cell transformation conditions for 5α-AD production. **a-b**. Effects of HP-β-CD/4-AD mass ratio (**a**) and Tween-80 concentration (**b**) on 5α-AD production. In panel a, the group with a 1:1 mass ratio was set as the control (100%). In panel b, the group with 0.05% Tween-80 was set as the control (100%). Data are presented as mean ± SD from three independent experiments (n=3). Statistical significance was analyzed by one-way ANOVA followed by Dunnett's test. *, $P<0.05$; **, $P<0.01$; ***, $P<0.001$ and ****, $P<0.0001$ indicate significant differences compared with the respective control groups; ns, not significant. **c-d**. Time courses of 5α-AD production at different initial 4-AD concentrations (**c**) and wet cell biomass (**d**).

Supplementary Files

This is a list of supplementary files associated with this preprint. Click to download.

- 0SupportingInformation.docx